Environmental Technology

ISSN: 0959-3330 (Print) 1479-487X (Online) Journal homepage: https://www.tandfonline.com/loi/tent20

Modelling the structure of sludge aggregates

Lech Smoczyński, Harsha Ratnaweera, Marta Kosobucka, Michał Smoczyński, Sławomir Kalinowski & Knut Kvaal

To cite this article: Lech Smoczyński, Harsha Ratnaweera, Marta Kosobucka, Michał Smoczyński, Sławomir Kalinowski & Knut Kvaal (2016) Modelling the structure of sludge aggregates, Environmental Technology, 37:9, 1122-1132, DOI: 10.1080/09593330.2015.1102332

To link to this article: https://doi.org/10.1080/09593330.2015.1102332

Published online: 07 Nov 2015.

ENVIRONMENTAL TECHNOLOGY, 2016
VOL. 37, NO. 9, 1122–1132
http://dx.doi.org/10.1080/09593330.2015.1102332

Taylor & Francis
Taylor & Francis Group

Modelling the structure of sludge aggregates

Lech Smoczyński[a], Harsha Ratnaweera[b], Marta Kosobucka[a], Michał Smoczyński[c], Sławomir Kalinowski[a] and Knut Kvaal[b]

[a]Department of Chemistry, Faculty of Environmental Management and Agriculture, University of Warmia and Mazury in Olsztyn, Olsztyn, Poland; [b]Department of Mathematical Sciences and Technology, Norwegian University of Life Sciences, Aas, Norway; [c]Department of Dairy Science and Quality Management, Faculty of Food Sciences, University of Warmia and Mazury in Olsztyn, Olsztyn, Poland

ABSTRACT

The structure of sludge is closely associated with the process of wastewater treatment. Synthetic dyestuff wastewater and sewage were coagulated using the PAX and PIX methods, and electrocoagulated on aluminium electrodes. The processes of wastewater treatment were supported with an organic polymer. The images of surface structures of the investigated sludge were obtained using scanning electron microscopy (SEM). The software *image analysis* permitted obtaining plots log *A* vs. log *P*, wherein *A* is the surface area and *P* is the perimeter of the object, for individual objects comprised in the structure of the sludge. The resulting database confirmed the 'self-similarity' of the structural objects in the studied groups of sludge, which enabled calculating their fractal dimension and proposing models for these objects. A quantitative description of the sludge aggregates permitted proposing a mechanism of the processes responsible for their formation. In the paper, also, the impact of the structure of the investigated sludge on the process of sedimentation, and dehydration of the thickened sludge after sedimentation, was discussed.

ARTICLE HISTORY
Received 27 March 2015
Accepted 1 September 2015

KEYWORDS
Coagulation; electrocoagulation; wastewater; sludge structure

1. Introduction

Agglomeration and aggregation [1] are natural phenomena. They are often used in food technology and in the chemical industry to produce, for example, polymers. The most important stage of wastewater coagulation is its hidden and fast hetero-flocculation [2], which leads to the formation of sludge aggregate-flocs [3,4,5]. Positively charged colloidal particles of Al or Fe hydroxide are attracting other negatively charged particles or molecules. Sedimentation or flotation and filtration [6] allow for the separation of the sludge from the treated wastewater. These processes allow for the recovery of, for example, phosphorus fertilizer, whose natural sources are close to depletion [7].

Image analysis is widely used in numerous scientific studies [8,9]. The structure of sludge is closely associated with the wastewater treatment process, so the course of coagulation–flocculation [3,10,11] or wastewater electrocoagulation [12–14] must permanently influence the resulting aggregate-flocs, even mechanisms of those processes differ from each other [15]. An advantage of electrocoagulation is also a possibility of disinfection of the wastewater treated [16]. In turn, the documented 'self-similarity' [17] of the objects representing parts of the sludge structure indicates their fractal characteristics [18] and enables a determination of their fractal dimension *D* [19–21]. The value *D* can determine not only the filling of space with mass but also the degree of surface jagging of the object. For example, if solid particles are filling the sphere completely, then $D = 3$; however, in case when only the cross-section of the sphere (circle) is filled, then $D = 2$. Porous objects with large specific surface areas are desirable in the so-called 'sweep flocculation' step [3], while compact and dense parts of sludge sediment are better and are more susceptible to self-dehydration.

A differentiation of the *D* value for different sludge components may be an indicator of the mechanism of their formation process [20–24]. The results of laboratory experiments [25] showing, for example, the impact of a coagulant dose of the mean *D* of post-coagulation aggregate-flocs [26] are known.

In the present study, the *D* values determined from the scanning electron microscopy (SEM) images of the sludge obtained during wastewater chemical coagulation or electrocoagulation, in both cases supported by an addition of organic polymer, were compared and discussed. The analysis of the database of obtained results enabled the following statement: 'the image of the sludge indicates the process of its formation'.

CONTACT Marta Kosobucka marta.kosobucka@uwm.edu.pl

2. Materials and methods

Samples of sewage from Rzeszel (PL, 5000pe) were collected for laboratory tests from a tank after initial mechanical treatment. Synthetic dyestuff wastewater was obtained by mixing an aqueous dye solution with a solution of KH_2PO_4.

Coagulation jar-tests were conducted at 21°C using a microprocessor-controlled jar-test type Kemira Flocculator 2000. The addition of coagulant was followed by a 2-minute rapid mixing at 400 rpm, and a slow mixing at 20 rpm. After 30 min of sedimentation, wastewater samples from the supernatant were collected for analyses. Colour, turbidity (TU), suspended solids (SS), total phosphorus (P_{total}) and COD were measured by a DR 2800 HACH-Dr Lange instrument system and pH was measured by a Hanna Instruments HI 8424 pH-meter. Two types of dyes for investigated wastewater were set: *red/orange* and *HACH*. The *red/orange* colour was measured spectrophotometrically at a wavelength of $\lambda = 430$ (*orange*) or 460 nm (*red*), providing maximum absorbance for aqueous solution of the dye. According to the calibration curve, it was expressed in mg of synthene red/orange per 1 L of wastewater. *HACH* is so-called 'apparent colour' of wastewater, and was determined using the HACH method at $\lambda = 455$ nm. The unit of apparent colour is 1 unit PtCo. Usually 1 unit of colour can be considered as 1 mg per 1 L. The unit of turbidity FTU (formazine turbidity unit) is equal to NTU. For this research, changes of colour and TU were the only parameters used for the indication of wastewater purification process. PIX-113 with 18 mg Fe/L and PAX-18 with 11 mg Al/L from Kemira were used as coagulants. An optimal constant dose of 0.105 ml/L of A_{100} polymer (also from Kemira) was used to assist the coagulation process.

Electrocoagulation tests were carried out on an experimental set-up constructed for the purpose [27]. A diagram of the electrocoagulation reactor with a recirculation system is presented in Figure 1(a).

A saturated NaCl solution (to increase specific conductance κ to 0.4 S/m) and 0.105 ml/L of A_{100} polymer were added to each 1 L of treated sewage. Electro-coagulated sewage was re-circulated between the electrolyser and the container. The process was performed at a constant current of $I = 0.1$ A and changes in voltage were continuously registered (Figure 1(b)). The direction of the current was alternated automatically every 256 s [28,29] to clean the electrodes. A sewage sample of 1 L was re-circulated within 64 min. The pH of the recirculating sewage was maintained at 6.0 by the addition a 2 M solution of HCl. Samples for analysis were collected every 5–15 min. Their colour, TU and SS were measured and the unused sample volumes were returned to the reactor

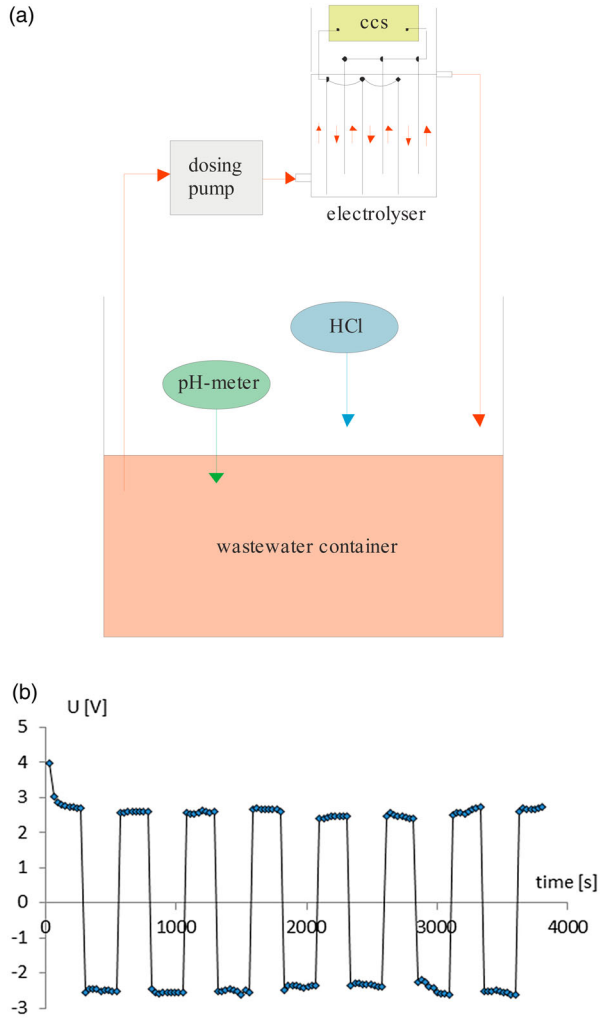

Figure 1. (a) Diagram of the electrocoagulation reactor and (b) change in the applied voltage.

to minimize changes in the system volume. P_{total} was determined only in the raw sewage and after the completion of electrocoagulation, because it was not possible to return the collected sample to the electrocoagulated system. A dosage of electrocoagulant was proportional to the time of electrolysis according to Faraday's law, $m = k \cdot i \cdot t$, where the electrochemical equivalent of aluminium is $k = 27/(96500 \cdot 3) = 9.3 \cdot 10^{-5}$ g·A^{-1}·s^{-1}.

The presence of red dyes in wastewater is particularly undesirable for the recipient environment. Therefore, two kinds of synthetic wastewater used in this research were obtained by mixing KH_2PO_4, NaCl and A_{100} polymer in water solution with the following dye: (a) Synten Red P-3BL or (b) Synten Orange P-4RL, respectively. It has already been proved that dyes without P–PO_4 are not susceptible to chemical coagulation or electrocoagulation [27], but the mixture combining the dyes with phosphate ions meant that they were highly sensitive to coagulation and electrocoagulation. Hence, 1 L of synthetic wastewater

contained 50 mg of the respective dye, 100 mg of P ($P–PO_4$), NaCl and 0.105 ml/L of A_{100} polymer. A wastewater sample of 1 L was recirculated like sewage within 64 min but at the higher $I = 0.3$ A. The sample's red colour was measured by spectrometry (using the research team's own calibration curve) at 460 nm and at 430 nm for red and orange, respectively, and transformed into the dye concentration. As with the tests with sewage, the unused sample volumes were returned to the reactor to minimize changes in system volume, and therefore P_{total} was determined only in the raw sewage and after the completion of electrocoagulation, because similar to sewage, it was not possible to return the collected sample to the electrocoagulated system. The applied doses of electrocoagulant nearly completely removed all of the total phosphorus and dye from the treated wastewater.

Finally, five types of sludge were obtained: two from sewage coagulation, one from sewage electrocoagulation and two from synthetic wastewater electrocoagulation. They were dried at 105°C (standard methods) at which any degradation of phosphorus compounds was not expected. Then a 1–2 mm fraction was separated on mesh screens and examined under a *Quanta FEG 250* Scanning Electron Microscope. Images from five sample locations (areas close to the four corners and the centre of the sample) were registered. Each of those five images was processed with an Image Analysis program (NIS-Elements Basic Research on Nikon). Thresholding was used and a binary image obtained. After a preliminary analysis of the images in NIS, the level of 105/106 was selected as the threshold limit because such conditions provided the clearest outline of the contours of the studied objects. This threshold level ensured maximal representativeness of jagged and uneven outlines and other morphological features of the analysed image. By clicking on a given white image, similar objects were automatically indicated in the analysed image. The selection of a white object was to eliminate all disturbances caused by black surface cracks, which were observed in selected images. The perimeter (P) and area (A) of medium and large objects were measured, and then log A vs. log P plots were obtained. As the analysed objects were self-similar, therefore their 'surface' fractal dimension D_a was calculated from the slope of the respective log $A = f$(log P) line [20,30]. The procedure is described in more detail in the Results and Discussion section.

3. Results and discussion

3.1. *Characteristics of treated wastewater*

Chemical treatment of the sewage by PAX is presented in Table 1. In the end, 100% of TU, approximately 90% of colour SS and P_{total} were removed from 1 litre of sewage treated with 38.6 mg Al from PAX.

The pH decreased from 7.9 (untreated sewage) to 7.53 (final treated). The sludge, now called '1–sewage/PAX' was obtained in that manner. Even half of this PAX dose resulted in 100% removal of TU, 87% of colour, almost 90% of SS and 80% of P_{total} from the sewage treated.

Chemical treatment of the sewage by PIX is presented in Table 2. Similar to PAX, 100% of TU, approximately 90% of colour, SS and P_{total} were removed from 1 L of sewage treated with 45.9 mg Fe from PIX.

The level of pH decreased from 7.9 (untreated sewage) to 7.40 (final treated). The sludge, now called '2–sewage/PIX' was formed in that manner. A bit more than half of this PIX dose resulted in 95% removal of TU, 80% of colour, 83% of SS and 73% of P_{total} from the sewage treated. Purification results achieved with PIX were a little worse compared to PAX, which was anticipated due to the slightly less molar dosage at a less favourable coagulation pH.

Electrocoagulation of the sewage is presented in Table 3. In the end, 100% of SS and TU, approximately 92% of colour and 95% of P_{total} were removed from 1 litre of sewage treated with $m = 9.3 \cdot 10^{-2} \cdot 3600 \cdot 0.1 =$ 33.48 mg Al.

Therefore, the sludge, now called '3–sewage/electro', was formed that way and the sample of it was taken out after 1800 seconds of sedimentation. Before the sedimentation, the quality of supernatant was worse – see the second-to-last line in Table 3. The results achieved here by sewage electrocoagulation appeared a little better compared to chemical coagulation.

Table 1. Sewage treated with PAX (1–sewage/PAX); primary $COD_0 = 1170 \rightarrow$ final $COD_f = 603$.

Al dose (mg/L)	Colour (mg/L)	SS (mg/L)	P_{total} (mg/L)	TU (NTU)	pH
0	4600	650	13.20	315	7.90
1.22	2260	320	10.20	132	7.73
4.90	1240	150	7.60	37	7.72
8.57	860	100	5.75	13	7.70
12.24	620	70	3.90	0	7.70
18.36	620	70	2.85	0	7.61
38.60	**480**	**50**	**1.55**	**0**	**7.53**

Table 2. Sewage 2 treated with PIX (2–sewage/PIX); primary $COD_0 = 1170 \rightarrow$ final $COD_f = 675$.

Fe dose (mg/L)	Colour (mg/L)	SS (mg/L)	P_{total} (mg/L)	TU (NTU)	pH
0	4600	650	13.20	315	7.90
3.67	2290	310	9.68	135	7.82
7.34	1770	240	8.55	79	7.82
11.01	1190	150	6.34	31	7.76
18.36	980	120	5.05	15	7.71
27.54	940	110	3.52	14	7.61
45.90	**520**	**50**	**1.58**	**0**	**7.40**

Table 3. Sewage 3 electrochemically treated (3–sewage/electro); primary $COD_0 = 527 \rightarrow$ final $COD_f = 305$.

Time (s)	TU (NTU)	Colour (mg/L)	SS (mg/L)	P_{total} (mg/L)	COD (mg/L)
0	237	3160	470	16.6	527
300	165	2670	380		
600	136	2350	320		
900	113	2130	280		
1200	96	1940	260		
1500	70	1610	210		
2400	39	1250	150		
3600	24	650	70		
After 1800 s of sedimentation	**0**	**265**	**0**	**0.86**	**305**

Table 4. Orange wastewater 4 electrochemically treated (4–orange/electro).

Time (s)	TU (NTU)	Dye conc. (mg/L)	SS (mg/L)	P_{total} (mg/L)
0	109	50	200	100
900	103	95	168	
1800	87	65	126	
2700	63	57	109	
3600	48	44	97	
After 1800 s of sedimentation	**1**	**6.1**	**12**	**7.1**

Electrocoagulation of the synthetic wastewater (orange) is presented in Table 4. In the end, almost 100% of TU, 94% of SS, 88% of dye and 93% of P_{total} were removed from 1 L of wastewater treated with $m = 9.3 \cdot 10^{-2} \cdot 3600 \cdot 0.3 = 100.44$ mg Al.

The Al dose here was 3 times higher (here $I = 0.3$ A) than with sewage electrocoagulation ($I = 0.1$ A). Therefore, the sludge, now called '4–orange/electro' was obtained in this manner and the sample was taken out after 1800 s of sedimentation. Before sedimentation, as in sewage (Table 3), the quality of supernatant was worse; see the second-to-last line in Table 4. The purification results achieved with sewage electrocoagulation (Table 3) were comparable to that achieved here (Table 4).

Electrocoagulation of the synthetic wastewater (red) is presented in Table 5. In the end, 100% of SS, 95% of TU, 93% of dye and 95% of P_{total} were removed from 1 L of wastewater treated the same as orange wastewater, then with $m = 9.3 \cdot 10^{-2} \cdot 3600 \cdot 0.3 = 100.44$ mg Al.

The sludge, now called '5–red/electro' was formed in that manner. According to expectations, before sedimentation the quality of supernatant was worse. Purification results achieved with sewage electrocoagulation (Table 3) and orange wastewater (Table 4) were comparable to that achieved here (Table 5).

Usually the polymer addition improved purification of both sewage and synthetic wastewater. The purification improvement also depends on the structure of obtained sludge particles, as their adsorption ability strongly depends on their specific surface area.

Table 5. Red wastewater 5 electrochemically treated (5–red/electro).

Time (s)	TU (NTU)	Dye conc. (mg/L)	SS (mg/L)	P_{total} (mg/L)
0	63	50	104	100
900	50	97	83	
1800	39	67	73	
2700	22	45	51	
3600	20	33	45	
After 1800 s of sedimentation	**3**	**3.5**	**0**	**4.9**

3.2. *Image analysis data and conversion*

Five selected regular images (Figure 2(a)) and five high-contrast images (Figure 2(b)) are presented in Figure 2. Similar SEM images were already described by Verma [31]. The images shown in line (a) of the photos were enhanced with maximum contrast and presented in line (b).

Then, the resulting images reveal clear contours of the shapes identifiable in the SEM photos.

Sewage images (1, 2 and 3) differ from the synthetic wastewater ones (4 and 5). The surface in images 4 and 5 (dye wastewater) is rather regular, while the surface in image 3 (sewage electrocoagulation) is particularly varying. Images 1 and 2 (chemical coagulation) are a bit similar to each other and differ much from image 3 (electrocoagulation). A small difference between image 1 (PAX) and 2 (PIX) can be attributed to the spherical shape of $\{Al(OH)_3\}$ colloidal particles and the rod-like and cylindrical shape of the $\{Fe(OH)_3\}$ particles [32,33]. Images 4 and 5 are characterized by minor structural differences.

The descriptions of the SEM images can be further developed, but this approach does not produce constructive or fundamental conclusions. The presence of jagged and uneven structures is difficult to quantify with the naked eye, and qualitative and quantitative comparisons supporting the classification of the analysed images into groups are impossible to perform. However, the NIS-Elements Basic Research software (Nikon, Japan) facilitates observations and the comparison of complex structures in the analysed images. This procedure emphasized certain characteristic shapes, traits and differences. Hence, the observed variations could be quantitatively confirmed in successive parts of this work.

The predominant size of the analysed objects and the subjective contrast of the images shown in Figure 2 did not affect self-similarity. The values of the determination coefficient are in the range of 0.95–0.98, therefore, self-similarity can be considered as statistical. The Image Analysis application measured area A and perimeter P for all objects. The resulting data were further used to

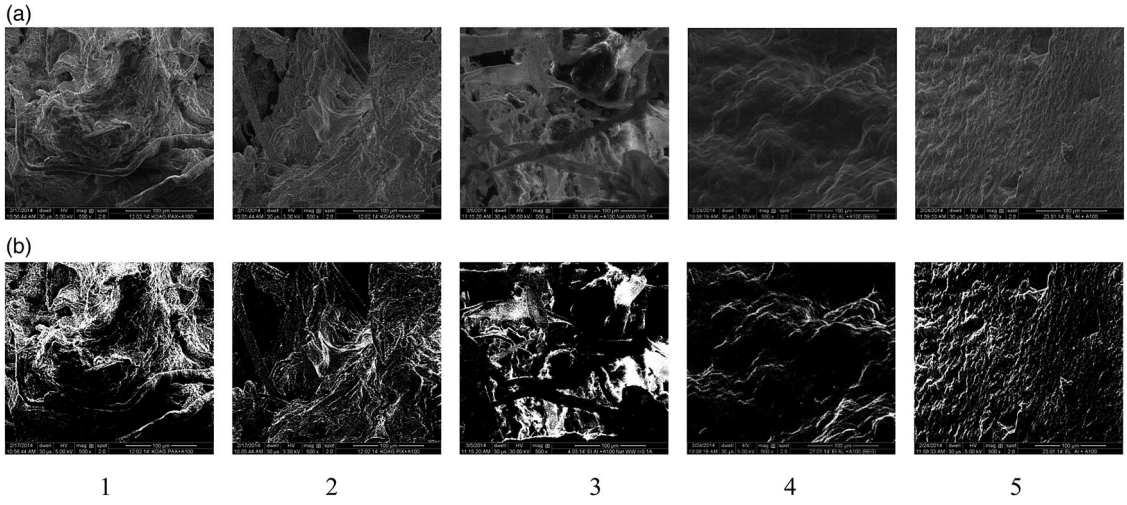

Figure 2. Selected examples of SEM images of five sludge types: (a) regular and (b) maximum contrast. 1–sewage/PAX, 2–sewage/PIX, 3–sewage/electrocoagulation, 4–orange/electrocoagulation, and 5–red/electrocoagulation.

develop log A vs. log P plots and charts illustrating the distribution of object dimensions.

Examples of log A vs. log P plots for five images, shown in Figure 2, are presented in Figure 3.

The direction coefficient values (1.02–1.13) in the equations on the graphs (Figure 3) indicated a low filling of the cross-section by mass, meaning that when the filling is complete, then $A = P^2$. They are accompanied by charts illustrating the distribution of R values (in μm) of surface objects to determine 'volume' fractal dimension D_v. The database in Figure 3 is described in detail in successive parts of this paper. It was also used in further calculations, simulations and models of sludge aggregate-flocs obtained by chemical coagulation and electrocoagulation.

The analysis was focused on objects characterized by significant variations in diameter size, from 29.7 to 71.2 μm. The range of variations in objects selected from the surface of the examined images seemed to be sufficient to ascertain the self-similarity of the analysed objects. The parameter that validates the significant self-similarity of the identified objects was the high value of determination coefficient R^2, which was calculated separately for every log A vs. log P plot. In all plots, R^2 always exceeded 0.95. This implies that the applied mathematical model of log $A = f(\log P)$ may fit the set of sludge images. The mean value of the slope (direction coefficient of the strait line equation) was further treated as 'area' fractal dimension D_a.

The mean value of D_a, together with standard deviation SD, is presented in Table 6.

The self-similarity of objects identified on the surface of the SEM images of sludge may indicate their fractal nature and structure. The accumulated data support the determination of surface fractal dimension D_a [30] for every group of analysed objects. Slope (slant) s determined for every log A vs. log P plot and raised to the power of 1.5 was further used as statistical extrapolation of surface fractal dimension D_a to volumetric fractal dimension D_v. It was assumed that flat jagged edges and uneven sludge surfaces can be 'extrapolated into space'. It was also assumed that D_v is only a statistical 'number', which is proportional to real fractal dimension D of aggregates forming the surface structure of the analysed sludge. In this sense, the value of D_v is not suitable for direct calculations, but it can be used to a *limited extent* in comparisons of the analysed object groups, that is, Al sludge and Fe sludge. The condensed structure of spherical Al sludge (higher D_v) and the jagged and porous structure of rod/wire-shaped Fe sludge (the lowest D_v) were thus mathematically validated again [27]. More condensed structures in sludge obtained by electrocoagulation compared to PAX sludge were noticed as the sewage electrocoagulation sludge appeared more compact than dye wastewater sludge.

3.3. *Structure of the analysed aggregates*

Coagulation and electrocoagulation of both sewage and synthetic wastewater creates agglomerates, aggregates and then finally the sludge flocs. The resulting aggregates contain colloidal particles of Al or Fe hydroxide and (a) P–PO_4, (b) organic polymer and/or (c) organic substances COD (sewage) or (d) dye D (synthetic wastewater). Other compounds such as NaCl and HCl contributed to a minor increase in the ionic strength of the solution. The unit for modelling aggregation–flocculation of sewage is presented schematically in Figure 4. Both negatively charged P–PO_4 and compounds responsible for COD were directly connected

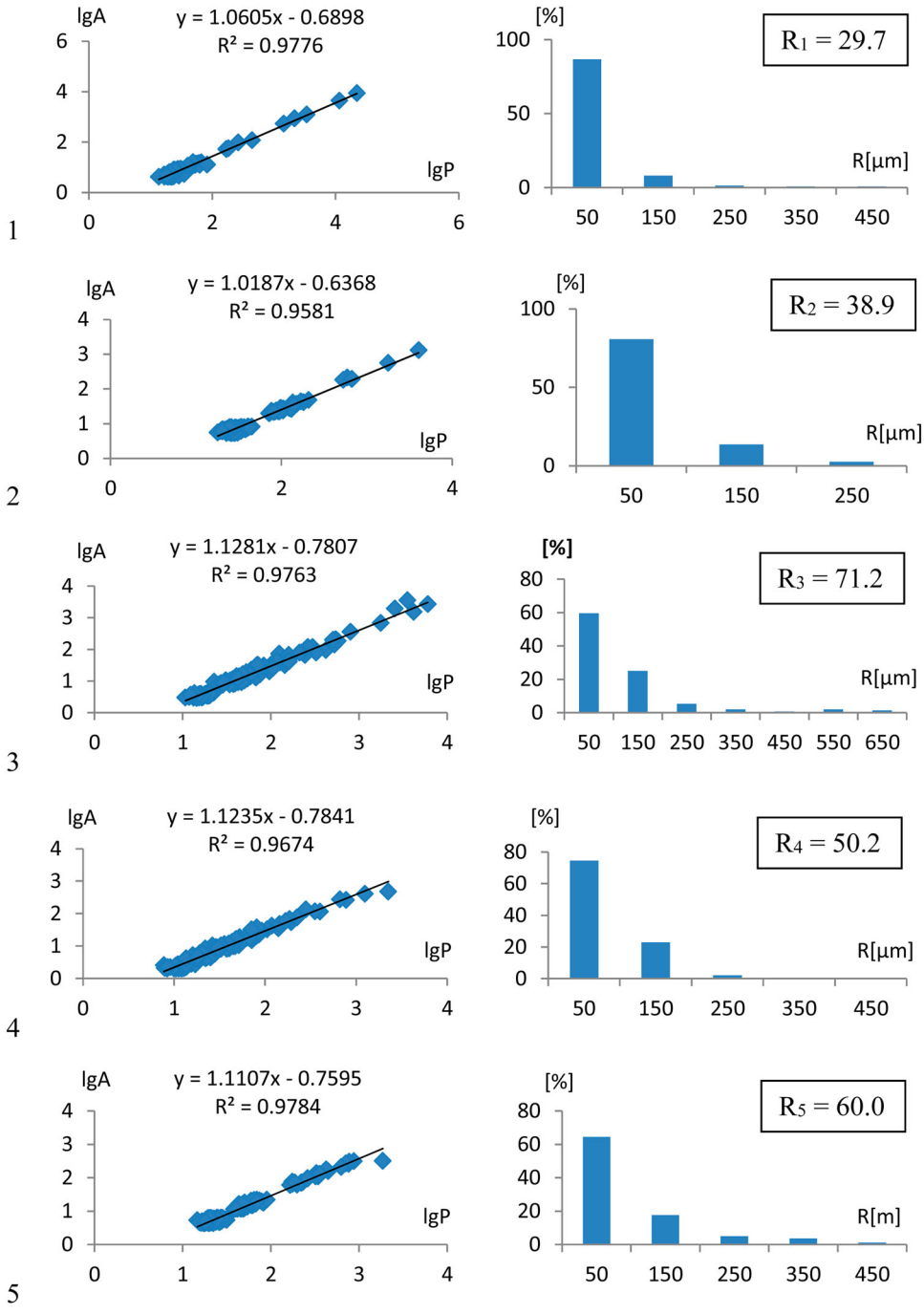

Figure 3. Selected examples (as in Figure 2) of *lg A ~ lg P* plots and distribution charts of five sludge types: 1–sewage/PAX, 2–sewage/PIX, 3–sewage/electrocoagulation, 4–orange/electrocoagulation, and 5–red/electrocoagulation.

Table 6. D_a – values, standard deviations of D_a and D_v – values.

WW type	1-sew/ PAX	2-sew/ PIX	3-sew/ electro	4-orange/ electro	5-red/ electro
D_a	1.0814	1.0244	1.1578	1.1068	1.1223
SD	0.0170	0.0075	0.0269	0.0116	0.0116
$D_v = D_a^{1.5}$	1.1246	1.0368	1.2461	1.1644	1.1889

to the surface of colloidal adsorbent $\{Al(OH)_3\}$ from PAX or Al-electrodes (electrocoagulation) or $\{Fe(OH)_3\}$ from PIX, respectively.

A schematic model for the aggregation/flocculation of sewage was proposed that is presented in Figure 4.

COD might form a direct bridge to the colloidal particle of $\{Al(OH)_3\}$ or $\{Fe(OH)_3\}$, while the polymer (P) might establish an indirect attraction by using up COD or $P–PO_4$ bridges. Compared to models described earlier [29], those models are a bit more complicated. The aggregates formed with the polymer support

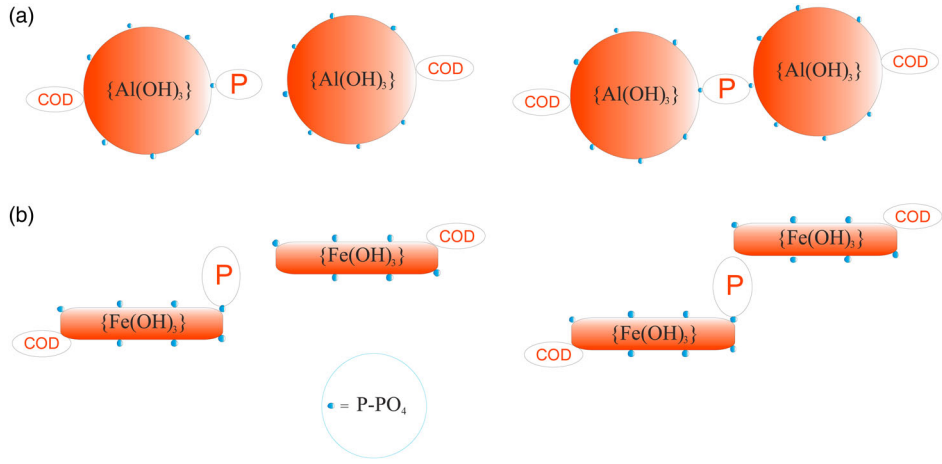

Figure 4. Sorption model of negatively charged P–PO_4 and COD from sewage on a positively charged colloidal hydroxide particle: (a) spherical Al and (b) cylindrical Fe.

might be larger because of the possibility of another indirect bridge, such as:

$$\{Al(OH)_3\} - [P - PO_4] - [P] - [P - PO_4] - \{Al(OH)_3\},$$
$$\{Fe(OH)_3\} - [P - PO_4] - [P] - [P - PO_4] - \{Fe(OH)_3\}.$$

A schematic model for the aggregation/flocculation of day wastewater was proposed that is presented in Figure 5.

In this case, a negatively charged P–PO_4 was directly connected to the adsorbent surface (as in Figure 4), but probably the positively charged dye had to be attracted to the adsorbent surface by P–PO_4 bridge like the COD was. A dye (D) could establish here a secondary indirect bridge by P–PO_4. Compared to models described earlier [27], those models are also more complicated. As with the models in Figure 4, the aggregates formed with the polymer support should be larger, although the possibility of an indirect bridge such as:

$$\{Al(OH)_3\} - [P - PO_4] - [D] - [P - PO_4] - \{Al(OH)_3\},$$
$$\{Fe(OH)_3\} - [P - PO_4] - [D] - [P - PO_4] - \{Fe(OH)_3\},$$

is rather excluded, with regard to the small size of the dye particle.

At pH < 6, colloidal particles of Al and Fe hydroxides and also a majority of hydrolysis species are positively charged [34]. The above $\{Al(OH)_3\}$ and $\{Fe(OH)_3\}$ (Figures 4 and 5) sols are stable due to electrostatic repulsion between particles, therefore they can start acting as colloidal adsorbents. The surface of adsorbent particles features negatively charged phosphate ions (Figures 4 and 5) and COD (Figure 4). Phosphate ions, in turn, can be covered with dye particles, therefore P–PO_4 forms

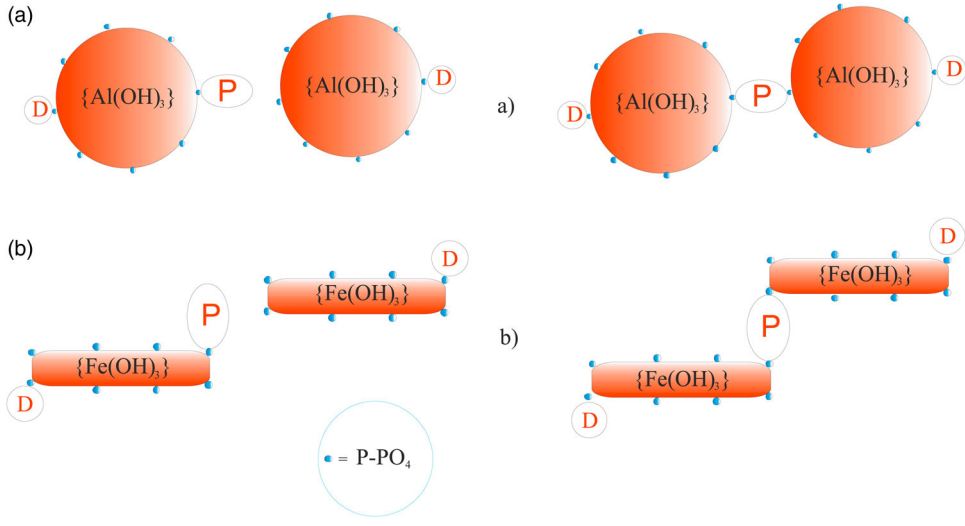

Figure 5. Sorption model of negatively charged P–PO_4 and dye *D* bridging to a positively charged colloidal hydroxide particle: (a) spherical Al and (b) cylindrical Fe.

probably a kind of bridge for a bit positive charged particle of dye, such as Synten Orange P-4RL and/or Synten Red P-3BL. As described previously [27], dye particles alone cannot be adsorbed on the surface of colloidal Al and Fe hydroxides. It was experimentally demonstrated many times that the addition of an aqueous solution of Al^{3+} or Fe^{3+} ions to an aqueous dye solution does not destabilize such a system, because coagulation and electrocoagulation do not take place, flocs are not formed in the system, and the red colour of the solution persists. However, such a system, only in the presence of phosphates, is easily destabilized by coagulation or electrocoagulation, and then dyes are completely removed from effluents. One explanation could be that the phosphate adsorbed on the surface of a colloidal adsorbent significantly compresses the electrical double layer responsible for the stability of the colloidal solution.

Phosphate ions, during a complexation or sorption process on colloidal sorbents of $\{Al(OH)_3\}$ or $\{Fe(OH)_3\}$ type, may destabilize these colloids, initiating the aggregation process. Such single aggregates as $\{Al(OH)_3\} - [P–PO_4]\}$ can agglomerate by indirect bridges, forming binary aggregates of $\{Al(OH)_3\} - [P–PO_4] - [D] - [P–PO_4] - \{Al(OH)_3\}$ type, which may be removed from the treated wastewater, for example, in the process of 'sweep flocculation'. Practically, during coagulation or electrocoagulation, always >90% of $P–PO_4$ and >90% of the dye pass from the liquid wastewater phase to the sludge.

Models of aggregates presented in Figures 4 and 5 may form a unit that can be theoretically considered a component of floc. Hence, the data from Figure 3 (size of aggregate) and Table 6 (fractal dimension) are used for calculating some statistical units of flocs responsible for the structure of the sludge obtained in this study:

(1) sewage/PAX $(29.67\ 1000\ nm/165\ nm)^{1.1246} = 342$ $\{Al(OH)_3\}$ aggregates,
(2) sewage/PIX $(38.9125\ 1000\ nm/165\ nm)^{1.0244} = 269$ $\{Fe(OH)_3\}$ aggregates,
(3) sewage/electrocoagulation $(71.22\ 1000\ nm/165\ nm)^{1.1246} = 1921$ $\{Al(OH)_3\}$ aggregates,
(4) orange/electrocoagulation $(50.24\ 1000\ nm/165\ nm)^{1.1644} = 780$ $\{Al(OH)_3\}$ aggregates,
(5) red/electrocoagulation $(60\ 1000\ nm/165\ nm)^{1.1889} = 1108$ $\{Al(OH)_3\}$ aggregates.

A comparison of the calculated numbers indicates that every volumetric unit of sewage/PIX (diameter ≈ 39 μm) contains only 269 aggregates, the sewage/PAX (diameter ≈ 30 μm) contains 342 aggregates, and the sewage/electrocoagulation (diameter ≈ 71 μm) contains as much as 1921 aggregates. Every volumetric unit of orange/electrocoagulation (diameter ≈ 50 μm) contains 780 and red/electrocoagulation (diameter ≈ 60 μm) 1108 aggregates. Therefore, the differences between the examined objects were quantified. The respective number of units in the analysed aggregates was extrapolated to the projection of a given aggregate-floc onto a plane:

(1) sewage/PAX $(342)^{0.66} = 47$ $\{Al(OH)_3\}$ aggregates,
(2) sewage/PIX $(269)^{0.66} = 40$ $\{Fe(OH)_3\}$ aggregates,
(3) sewage/electrocoagulation $(1921)^{0.66} = 147$ $\{Al(OH)_3\}$ aggregates,
(4) orange/electrocoagulation $(780)^{0.66} = 81$ $\{Al(OH)_3\}$ aggregates,
(5) red/electrocoagulation $(1108)^{0.66} = 102$ $\{Al(OH)_3\}$ aggregates.

Spherical $\{Al(OH)_3\}$ aggregates and cylindrical $\{Fe(OH)_3\}$aggregates were further arranged in a circle with a suitable diameter proportional to its size and succeeding models are presented in Figure 6. Five different structures of cluster-units of the sewage and wastewater flocs (described in Figure 3 and in Table 6) are presented schematically in Figure 6.

As the quality and structure of sludge seems to be an important technological parameter, therefore the structure of analysed sludge objects was simulated with model $\{Al(OH)_3\}$ colloidal particles with average diameter of $R = 165$ nm proposed by Macedo [35] and cylindrical $\{Fe(OH)_3\}$ particles. Due to an absence of uniform data regarding the size of $\{Fe(OH)_3\}$ cylinders [32–33], the length of a colloidal $\{Fe(OH)_3\}$ particle equal to the diameter of a spherical $\{Al(OH)_3\}$ particle, that is, 165 nm, was used both in this modelling and in further calculations. As not enough data were obtained to prove the bridges:

$$\{Al(OH)_3\} - [P - PO_4] - [P] - [P - PO_4] - \{Al(OH)_3\},$$
$$\{Fe(OH)_3\} - [P - PO_4] - [P] - [P - PO_4] - \{Fe(OH)_3\},$$

they were not considered in the cluster-units modelling, although some further considerations indicate such a possibility.

The distribution charts in Figure 3 indicate an average size in the width, ranging from 29.7 μm (1–sewage/PAX) to 71.2 μm (3-sewage/electrocoagulation) for the modelled cluster-units presented in Figure 6. Contrary to previous models arranged in a circle with the same diameter [25,27], here the modelled cluster-units are contained in their real circle, according to their real size. Therefore, Figure 6 shows a larger cluster-unit of flocs obtained by electrocoagulation than those formed in chemical coagulation. A little larger cluster-unit at PIX than at PAX application is observed, as a larger cluster-unit for sewage electrocoagulation was modelled compared to the cluster-unit obtained from dye wastewater electrocoagulation. Compared to previous data obtained with

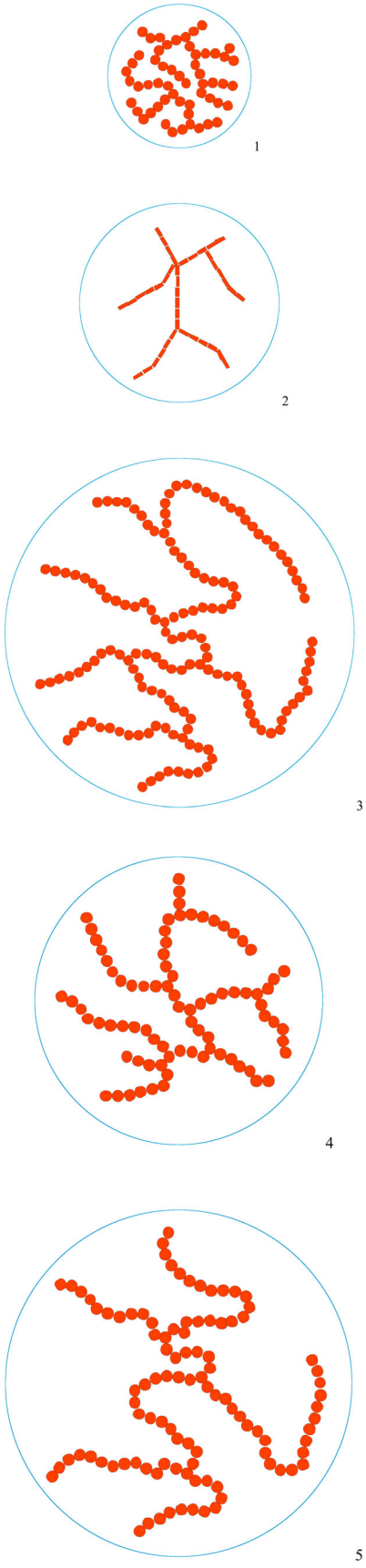

Figure 6. Estimated structure of a cluster-unit: 1–sewage/PAX, 2–sewage/PIX, 3–sewage/electrocoagulation, 4–orange/electrocoagulation, 5–red/electrocoagulation.

no polymer application [27,29], here the variation of cluster-unit sizes in general is much higher. The sizes of the cluster-units of sludge obtained by chemical coagulation (sewage/PAX and sewage/PIX) is approx. two times less than those obtained without polymer [27,29], but the sizes of the cluster-units obtained by electrocoagulation are close to those without a polymer. A few times, a lower number of particles in every cluster-unit were responsible for much lower D_v values. There are two possible explanations for that:

(a) some 'dimers' like $\{Al(OH)_3\}$ – [P–PO_4] – [P] – [P–PO_4] – $\{Al(OH)_3\}$ and/or $\{Fe(OH)_3\}$ – [P–PO_4] – [P] – [P–PO_4] – $\{Fe(OH)_3\}$ were involved into the cluster-unit formation,

(b) the cluster-units obtained with polymer support were swelling with water.

If (a), then a more compact structure of cluster-units formed with larger particles (dimers) can be expected. If (b), then more troubles involved in dewatering such sludge can be expected. Similar sizes of electrocoagulation cluster-units obtained both without and with the use of polymer and a higher number of particles per cluster-unit may indicate less of an effect of polymer on electrocoagulation of wastewater compared to chemical coagulation. An explanation of this phenomenon could be the availability of polymer in those processes. Anode dissolution in electrocoagulation is only a surface process, when less availability of polymer is noticed, while chemical coagulation runs in all volumes, when polymer can be more engaged. The anodic process in the system is Al dissolution, according to the equation: $Al^0 \rightarrow Al^{3+} + 3e^-$.

In general, the quality and structure of various types of sludge can be compared quantitatively based on the determined values of fractal dimension D_v of aggregates in a given cluster-unit and also on the given cluster-unit size. The variations in the value of D_v are determined by at least three principal sludge parameters: (a) sorption capacity [1,3], (b) susceptibility to sedimentation or floating [24] and (c) susceptibility to dehydration. Sludge aggregates with well-developed and jagged surface structures are therefore characterized by a lower value of D_v, and have a greater ability to adsorb pollutants during sweep flocculation [1,3] than aggregates characterized by a more compact structure (higher value of D_v and smaller specific surface area). Sludge formed by aggregates with a lower value of D_v should be easier to separate from the phase of effluents treated by flotation than sedimentation. In theory, sludge with lower D_v should be less susceptible to dehydration or even 'self-dehydration' [17], than sludge with higher D_v. This observation is debatable, as Waite [24] argued that SO_4^{2-} ions present in PIX are responsible for the 'structural'

decomposition of sludge flocs and that 'looser' aggregates support filtration (sludge separation) and dehydration of filtered sludge.

Another important parameter of the examined sludge is the size of its cluster-unit. These units may determine a floc's structure. Small and dense cluster-units obtained from sewage treated with PAX should form compact flocs, which leads to a low water content and therefore easier dewatering process. Still small but less dense cluster-units (lower D) obtained from the sewage treated with PIX probably contain more water. Earlier research has showed [36] that pre-polymerized coagulants (PAX) favour the 'adsorption-charge neutralization' mechanism, which warrants more efficient purification of effluents. Electrocoagulation of both the sewage and the synthetic (dye) wastewater forms a larger cluster-unit than chemical coagulation. The loose structure of flocs formed by such cluster-units can be expected here, even high values of D in the aggregates creating those cluster-units. Considering both: (a) the fractal dimension D of the aggregate and (b) size of the cluster-units makes possible the sludge description and characterization.

4. Conclusions

The applied image analysis method proved that the examined wastewater sludge was composed of self-similar aggregate-flocs with fractal properties, and hence log A vs. log P plots (A – area, P – perimeter) supported the determination of surface fractal dimension D_a. SEM images and the value of volumetric fractal dimension D_v (extrapolated from D_a) quantitatively described sludge aggregate-flocs. Sludge aggregates obtained with polymer support contained substantially fewer particles than those obtained without polymer. Our experiment revealed again that phosphate ions are required for the destabilization of colloid-dye systems. A model for P–PO_4, COD and dye sorption on a colloidal sorbent comprising $Al(OH)_3$}, {$Fe(OH)_3$} and polymer was developed. The technological consequences of the impact exerted by D_v of aggregates and size of cluster-unit on sweep flocculation, effluent separation and dehydration were defined based on a graphic simulation of cluster-unit made of {$Al(OH)_3$} and {$Fe(OH)_3$} particles. Both, fractal dimension D of the aggregate and the size of the cluster-unit make possible the sludge description and characterization.

Disclosure statement

No potential conflict of interest was reported by the authors.

Funding

The research leading to these results has received funding from the Polish-Norwegian Research Programme operated by the National Centre for Research and Development under the Norwegian Financial Mechanism 2009–2014 in the framework of Project Contract No. POL-NOR/196364/7/2013.

References

[1] Yu W, Liu T, Gregory J, Li G, Liu H, Qua J. Aggregation of nano-sized alum–humic primary particles. Sep Purif Technol. 2012;99:44–49.
[2] Yang G, Biswas P. Computer simulation of the aggregation and sintering restructuring of fractal-like clusters containing limited numbers of primary particles. J Colloid Interface Sci. 1999;211:142–150.
[3] Duan J, Gregory J. Coagulation by hydrolyzing metal salts. Adv Colloid Interface Sci. 2003;100–102:475–502.
[4] Smoczynski L, Mroz P, Wardzynska R, Załeska-Chrost B, Dłuzynska K. Computer simulation of flocculation of suspended solids. Chem Eng J. 2009;152:146–150.
[5] Kallay N, Žalac S. Introduction of the surface complexation model into the theory of colloid stability. Croat Chem Acta. 2001;74(3):479–497.
[6] Zodi S, Potier O, Lapicque F, Leclerc JP. Treatment of the textile wastewaters by electrocoagulation: effect of operating parameters on the sludge settling characteristics. Sep Purif Technol. 2009;69:29–36.
[7] Cordell D, Drangert JO, White S. The story of phosphorus: global food security and food for thought. Global Environ Change. 2009;19:292–305.
[8] Prats-Montalban JM, Ferrer A, Bro R, Hancewicz T. Prediction of skin quality properties by different multivariate image analysis methodologies. Chemometr Intell Lab. 2009;96:6–13.
[9] Szponder DK, Trybalski K. Application of computer image analysis and scanning electron microscopy in environmental engineering and waste management. Chall Mod Technol. 2011;2(2):56–62.
[10] Smoczynski L, Wardzynska R, Pierozynski B. Computer simulation of polydispersive sol coagulation process. Can J Chem Eng. 2013;91:302–310.
[11] Smoczynski L, Bukowski Z, Wardzynska R, Załeska-Chrost B, Dłuzynska K. Simulation of coagulation, flocculation and sedimentation. Water Environ Res. 2009;81(4):348–356.
[12] Butler E, Hung Y-T, Yu-Li Yeh R, Al Ahmad MS. Electrocoagulation in wastewater treatment. Water. 2011;3:495–525.
[13] Irdemez S, Demircioglu N, Yıldız YS, Bingul Z. The effects of current density and phosphate concentration on phosphate removal from wastewater by electrocoagulation using aluminum and iron plate electrodes. Sep Purif Technol. 2006;52:218–223.
[14] Secula MS, Cretescu I, Petrescu S. An experimental study of indigo carmine removal from aqueous solution by electrocoagulation. Desalination. 2011;277:227–235.
[15] Zaleschi L, Teodosiu C, Cretescu I, Rodrigo MA. A comparative study of electrocoagulation and chemical coagulation

processes applied for wastewater treatment. Environ Eng Manag J. 2012;11(8):1517–1525.
[16] Zaleschi L, Saez C, Canizares P, Cretescu I, Rodrigo MA. Electrochemical coagulation of treated wastewaters for reuse. Desalin Water Treat. 2013;51(16–18):3381–3388.
[17] Smoczynski L. Aggregation of the silica suspension by alcoagulants. Pol J Chem. 2000;74:1617–1624.
[18] Jullien R, Meakin P. Simple models for the restructuring of 3-dimensional ballistic aggregates. J Colloid Interface Sci. 1989;127:265–272.
[19] Mandelbrot BB. The fractal geometry of nature. San Francisco, CA: Freeman; 1982.
[20] Meng FG, Zhang HM, Li YS, Zhang XW, Yang FL, Xiao JN. Cake layer morphology in microfiltration of activated sludge wastewater based on fractal analysis. Sep Purif Technol. 2005;44:250–257.
[21] Zhao YQ. Settling behaviour of polymer flocculated water-treatment sludge II: effects of floc structure and floc packing. Sep Purif Technol. 2004;35:175–183.
[22] Meakin P. The effects of reorganization processes on two-dimensional cluster – cluster aggregation. J Colloid Interface Sci. 1986;112:187–194.
[23] Pastor-Satorras R, Rubí JM. Particle-cluster aggregation with dipolar interactions. Phys Rev E. 1995;51(6):5994–6003.
[24] Waite TD. Measurement and implications of floc structure in water and wastewater treatment. Colloid Surface A. 1999;151:27–41.
[25] Yang Z, Yang H, Jiang Z, Huang X, Li H, Li A, Cheng R. A new method for calculation of flocculation kinetics combining Smoluchowski model with fractal theory. Colloid Surface A. 2013;423:11–19.
[26] Smoczynski L, Wardzynska R. Study on macroscopic aggregation of silica suspension and sewage. J. Colloid Interface Sci. 1996;183:309–314.
[27] Smoczynski L, Ratnaweera H, Kosobucka M, Smoczynski M. Image analysis of sludge aggregates. Sep Purif Technol. 2014;122:412–420.
[28] Smoczynski L, Munska KT, Pierozynski B, Kosobucka M. Electrocoagulation of model wastewater using aluminium electrodes. Pol J Chem Technol. 2012;14(3):66–70.
[29] Smoczynski L, Munska K, Pierozynski B. Electrocoagulation of synthetic wastewater. Water Sci Technol. 2013;67 (2):404–409.
[30] Dziuba J, Babuchowski A, Smoczynski M, Smietana Z. Fractal analysis of caseinate structure. Int Dairy J. 1999;9:287–292.
[31] Verma S, Prased B, Mishra IM. Pretreatment of petrochemical wastewater by coagulation and the sludge characteristics. J Hazard Mater. 2010;178:1055–1064.
[32] Haas W, Zrinyi M, Kilian HG, Heise B. Structural analysis of anisometric colloidal iron(III)-hydroxide particles and particle-aggregates incorporated in poly(vinyl-acetate) networks. Colloid Polym Sci. 1993;271:1024–1034.
[33] Rohrsetzer S, Paszli I, Csempesz F, Ban S. Colloidal stability of electrostatically stabilized sol particles. Part I: The role of hydration in coagulation and repeptization of ferric hydroxide sol. Colloid Polym Sci. 1992;270:1243–1251.
[34] Amirtharajah A, Mills MK. Rapid-mix design for mechanism of alum coagulation. J AWWA. 1982;74:210–216.
[35] Macedo MIF, Osawa CC, Bertran CA. Sol-gel synthesis of transparent alumina gel and pure gamma alumina by urea hydrolysis of aluminum nitrate. J Sol-Gel Sci Technol. 2004;30:135–140.
[36] Ratnaweera H, Fettig J, Ødegaard H. Particle and phosphate removal mechanisms with prepolymerized aluminum coagulants. In: Hahn HH, Klute R. editor. Chemical water and wastewater treatment II: Berlin: Springer-Verlag; 1992. p. 3–17.